



IRZAL NUR¹, PAULINA TABA², ARIFUDIN IDRUS³, ULVA RIA IRFAN⁴,
SUFRIADIN SUFRIADIN⁵, SRI WIDODO⁶, ARYANTI VIRTANTI ANAS⁷,
MUHAMMAD RIDHA ARDIAN⁸, ADELIA DWIRISA ANJELINA⁹

The genesis and potential utilization of zeolite in the Moncongloe Area, Maros, South Sulawesi, Indonesia

Introduction

In the Moncongloe area, Maros Regency, South Sulawesi Province, Indonesia, zeolite mineralization in porphyritic rhyolite and green tuff was identified in a volcano-sedimentary sequence that was exposed as a result of rock (building materials) mining activity. Geologically, the Moncongloe area is included in the Camba Formation (*Tmc*) which is arranged by units of marine sedimentary rocks interbedded with volcanics. The lithology units in the formation consist of tuff, sandstone and claystone, with intercalations of marl, limestone,

✉ Corresponding Author: Irzal Nur Nur; e-mail: irzal.nur@eng.unhas.ac.id

¹ Mining Engineering Department, Faculty of Engineering, Hasanuddin University, Indonesia;
e-mail: irzal.nur@eng.unhas.ac.id

² Chemistry Department, Faculty of Mathematics and Natural Sciences, Hasanuddin University, Indonesia;
ORCID iD: 0000-0001-7327-5505; Scopus ID: 56554043300; e-mail: paulinatoba@unhas.ac.id

³ Geological Engineering Department, Faculty of Engineering, Gadjah Mada University, Indonesia;
ORCID iD: 0000-0003-4083-4811; Scopus ID: 16642483700; e-mail: arifidruss@ugm.ac.id

⁴ Geological Engineering Department, Faculty of Engineering, Hasanuddin University, Indonesia;
ORCID iD: 0000-0002-4167-6766; Scopus ID: 56964494400; e-mail: ulvairfan@unhas.ac.id



volcanic conglomerate and breccia, as well as coal, which varies in color, is mostly well consolidated and bedding of 4 to 100 cm in thickness. Tuffs are fine to lapilli in size, red clayey tuff contains abundant biotite, conglomerate and breccia is composed of andesite and basalt pebbles of 2 to 30 cm in size, sandy limestone contains fragments of coral and mollusc, dark gray claystone and marl contain small forams and coal intercalation is 40 cm thick (Sukanto and Supriatna 1982). The zeolite mineralization occurs in the tuff member of the Camba Formation (Figures 1 and 2).

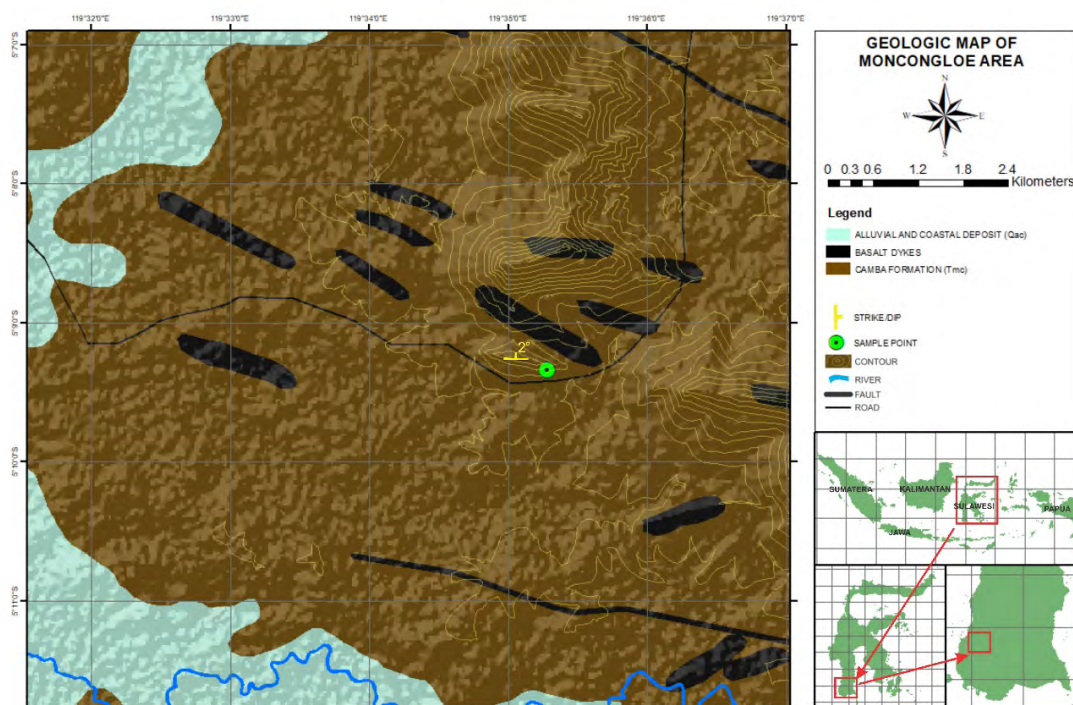


Fig. 1. Geologic map of Moncongloe area and surrounding (modified from Sukanto and Supriatna 1982).
The sampling point is shown, situated in the Camba Formation

Rys. 1. Mapa geologiczna obszaru Moncongloe i okolic (zmodyfikowana na podstawie Sukanto i Supriatna 1982).
Pokazano punkt poboru próbek położony w formacji Camba

⁵ Mining Engineering Department, Faculty of Engineering, Hasanuddin University, Indonesia;
ORCID iD: 0000-0002-6103-3143; e-mail: sufriadin_as@yahoo.com

⁶ Mining Engineering Department, Faculty of Engineering, Hasanuddin University, Indonesia;
ORCID iD: 0000-0001-8613-9107; Scopus ID: 25824547400; e-mail: srwd007@yahoo.com

⁷ Mining Engineering Department, Faculty of Engineering, Hasanuddin University, Indonesia;
Scopus ID: 56963743400; e-mail: aryantiv@unhas.ac.id

⁸ Mining Engineering Department, Faculty of Engineering, Hasanuddin University, Indonesia;
e-mail: muhammadridhaardian@gmail.com

⁹ Mining Engineering Department, Faculty of Engineering, Hasanuddin University, Indonesia;
e-mail: adeliadwirisaa@gmail.com



Fig. 2. Outcrop of volcano-sedimentary sequence containing light green layer of 6.8 m zeolite-bearing porphyritic rhyolite (A) and green tuff (B) in the Moncongloe area

Rys. 2. Wychodnia sekwencji wulkaniczno-osadowej zawierająca jasnozieloną warstwę 6,8 m zawierającego zeolit ryolitu porirytycznego (A) i tufu zielonego (B) w rejonie Moncongloe

Genetically, zeolite mineral deposits can be formed from volcanic ash sedimentation processes in alkaline lake environments, groundwater alteration results, diagenetic processes (low-grade metamorphism) and hydrothermal processes. The genetic types that are commonly found are those formed in tuffaceous rocks, where zeolite is formed from the sedimentation of volcanic ash that has undergone an alteration process; here a reaction occurs between fine-grained, rhyolitic acid tuff and pore or meteoric water (Cicerali et al. 2020; Mormone and Piochi 2020; Suliman et al. 2022).

Zeolite minerals are hydrated alumino-silicate compounds with their main elements consisting of alkaline and alkaline earth cations. This compound has a three-dimensional structure and has pores that can be filled by water molecules. Based on their mineralogy, chemical composition, and crystal structure, zeolites have three distinctive characteristics which are closely related to their uses as industrial minerals, including as:

- a) absorbents – zeolites can absorb certain molecules due to the water molecules in the structure cavity that have evaporated through temperature increasing;
- b) ion exchangers – zeolites can exchange ions due to the displacement event between Si^{4+} and Al^{3+} ions;
- c) molecular sieves – zeolites can enrich or select the molecules to be absorbed because the diameter of the structure cavity of each type of zeolite is specific and only the proper ones can be absorbed.

Based on their mineralogical and chemical characteristics, zeolite minerals can be utilized in various fields, including in agriculture and plantation, in farming and fisheries, in gas drying and purification, as filler, as ceramic material, in coal gasification, in the petroleum industry, in the utilization of solar energy, in environmental sustainability, in the aircraft industry, in water purification, in photography, and in radioactive fields (Suwardi 2002; Auerbach et al. 2003; Erdem et al. 2004; Moshoeshoe et al. 2017; Buzimov et al. 2018; Asselman et al. 2022; Pellens et al. 2022).

This paper describes a recent study of the zeolite mineralization in the Moncongloe area on the basis of field and laboratory data, which focused on its genetic aspects and potential utilizations based on its mineralogical and chemical characteristics.

1. Sampling and methods

In this study, the field works were conducted in the outcrops of volcano-sedimentary sequence in the Moncongloe area (Figure 2), where zeolite-bearing as well as volcanic and sedimentary rocks samples were systematically collected from each layer, namely (from bottom to top) claystone, coal, shale, porphyritic rhyolite, green tuff, tuff, red claystone, reddish shale, and reddish claystone. In the field, the zeolite mineral itself was mainly recognized in porphyritic rhyolite and green tuff layers, with thicknesses of 4.5 and 2.3 m, respectively, and a total of 6.8 m. Strike/dip orientation of the stratigraphic sequence, measured in shale, is N275°E/2°. During the field works, twelve samples were collected from the outcrops. The locations and sample codes are shown in Figure 3.

Of the twelve samples, five samples were selected for analysis in the laboratory, namely four samples of zeolite-bearing porphyritic rhyolite (sample code MZ-1D1, MZ-1D2, MZ-1D3, MZ-1D4) and one sample of green tuff (sample code MZ-2A). This is based on the consideration that in the field (on hand specimen samples) the porphyry rhyolite rock clearly showed a content of zeolite. In green tuff, indications of a zeolite content were not clearly detected in outcrops or hand specimens, but because the hydrothermal environment green tuff generally contain zeolite, one sample was also analyzed.

The laboratory works include mineralogical analysis (petrography and XRD) and bulk chemical analysis (XRF for major oxides, ICP-OES and ICP-MS for trace elements). Sample preparations for petrographic analysis in the form of thin sections as well as their observations using Nikon 140c type polarizing microscope were performed in the Optical Mineral Laboratory, Department of Geological Engineering, Hasanuddin University. For the XRD analysis, five selected powdered samples of zeolite-bearing porphyritic rhyolite and green tuff were scanned using a Shimadzu Maxima_X XRD-7000 X-Ray diffractometer machine. The diffraction patterns were recorded with scanning stage of 5 to 70° 2-theta. Results of the XRD scanning were then analyzed using the PDX-2 program issued by the Mineral Data Institute (MDI) combined with Impact Match! Version-3 software, to identify mineral species contained in the samples. The whole stages of the XRD works, from sample preparation,

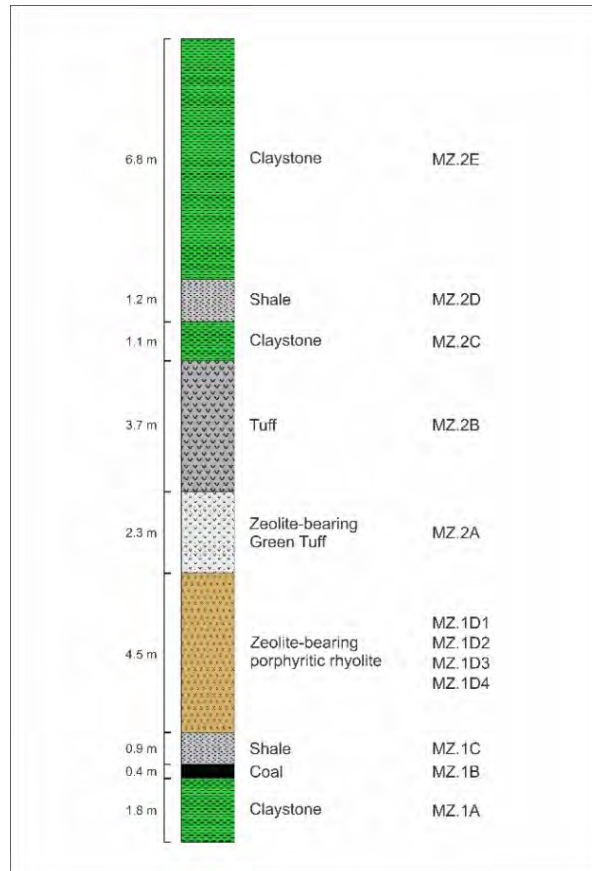


Fig. 3. Overall lithological profile of the outcrops also showing the position of each collected sample

Rys. 3. Ogólny profil litologiczny wychodni, pokazujący także położenie każdej pobranej próbki

scanning, analysis, and the interpretation and identification of minerals were conducted in the XRD Laboratory, Department of Mining Engineering, Hasanuddin University.

For chemical analysis, the rest of the five powdered samples were sent to the PT. Intertek Utama Services commercial research laboratory, Jakarta, Indonesia, to measure their chemical composition. Major elements were measured by X-ray fluorescence spectroscopy (XRF), while trace elements were measured by inductively coupled plasma (ICP) methods. The XRF test performed on ten main oxides plus LOI (total volatile substances) from the analyzed rocks, specifically SiO_2 , TiO_2 , Al_2O_3 , Fe_2O_3 , MnO , CaO , MgO , Na_2O , K_2O and P_2O_5 . The analysis results of the main elements in the petrogenesis were used to perform the classification, grouping and naming of rocks. Dissolved trace and rare earth elements were analyzed by inductively coupled plasma mass spectrometry (ICP-MS, agilent technologies type 7700) and inductively coupled plasma optical emission spectroscopy

(ICP-OES, agilent technologies type 725). The accuracy of the results was obtained by analyzing certified reference material (ICP Standard Solution by Kanto Chemical Co., Inc. and ICP multi-element standard solution VI by Merck KGaA, Darmstadt). All samples were blank corrected and duplicated to assess the reproducibility. The sample preparation for total metal analysis includes digesting the samples with four acids (HCl, HClO₄, HNO₃, and HF). Measured REEs abundances were normalized against chondrite (McDonough and Sun 1995).

2. Results and discussion

2.1. Mineralogical characteristics

In general, in hand specimen (sample MZ-2A), porphyritic rhyolite samples show a greenish gray color, composed of K-feldspar phenocrysts, less fine biotite crystals scattered in sparse spaces, and plagioclase groundmass (Figure 4). The green tuff samples are fine-grained, composed of volcanic crystals and glass. Four porphyritic rhyolite samples (sample code MZ-1D1, MZ-1D2, MZ-1D3, MZ-1D4) and one green tuff sample (sample code MZ-2A) were observed under the microscope and analyzed using the XRD method.

Observation under the microscope shows the presence of K-feldspar (orthoclase), plagioclase, and less biotite. K-feldspar and plagioclase phenocrysts have been altered to philipsite-type zeolite, while fine feldspar crystals have been altered to smectite (Figure 5).



Fig. 4. Hand specimen sample MZ-2A

Rys. 4. Próbkę ręczna MZ-2A

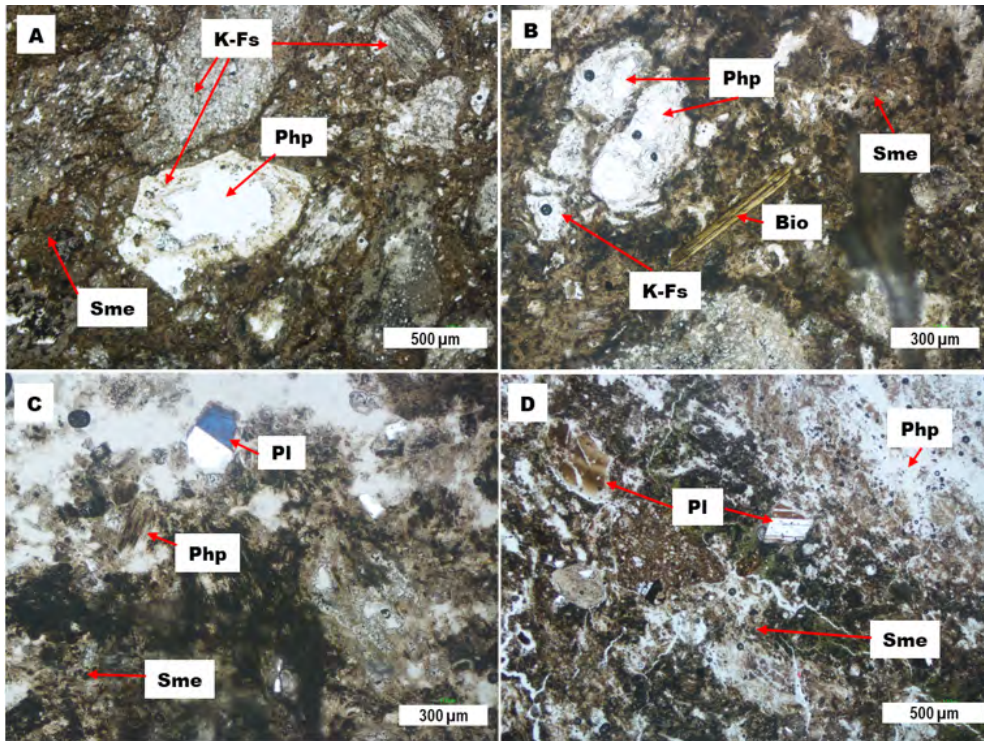


Fig. 5. Photomicrographs of zeolite-bearing rock samples. (A, B). K-feldspar (K-Fs) presents as phenocrysts within the porphyritic rhyolite, phillipsite (Php) and smectite (Sme) are alteration products of feldspar, biotite also appeared. MZ-1D1; crossed nicols. (C, D). Plagioclase occurs as phenocrysts and mostly primary minerals have been altered to phillipsite and smectite. MZ-1C; crossed nicols

Rys. 5. Fotomikrografie próbek skał zeolitowych. (A, B). K-skalenie (K-Fs) występują jako fenokryształy w porfirowym ryolicie, filipsyt (Php) i smektyt (Sme) są produktami przemian skalenia, pojawił się także biotyt. MZ-1D1; skrzyżowane nicole. (C, D). Plagioklaz występuje w postaci fenokryształów, a większość minerałów pierwotnych została zmieniona w filipsyt i smektyt. MZ-1C; skrzyżowane nicole

Results of XRD analysis on the five samples also show the presence of the minerals phillipsite and smectite, together with feldspar, quartz and calcite (Figure 6).

2.2. Chemical characteristics

The five samples that had been analyzed mineralogically were also analyzed chemically using the XRF method for the major elements, as well as ICP-OES and ICP-MS for the trace elements. The results are presented in Table 1.

It can be seen in Table 1 that in general, the chemical composition of the important elements characterizing zeolite minerals, especially aluminum and potassium (Al and K),

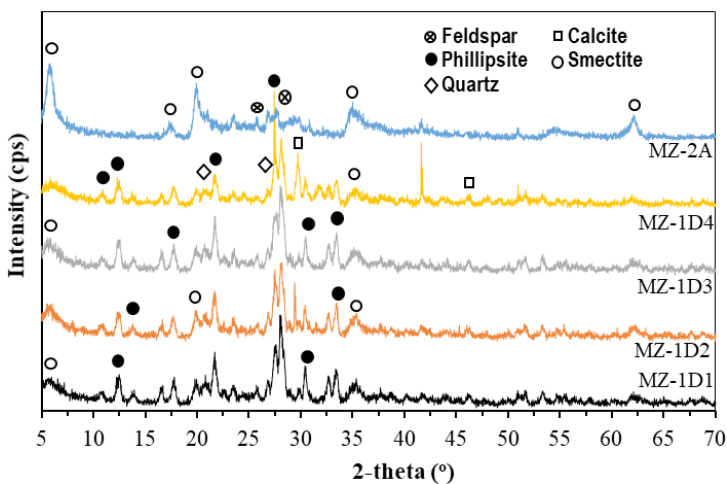


Fig. 6. X-ray diffractograms of the five samples

Rys. 6. Dyfraktogramy rentgenowskie pięciu próbek

Table 1. Results of chemical analysis

Tabela 1. Wyniki analizy chemicznej

| Sample Code | MZ-1D1 | MZ-1D2 | MZ-1D3 | MZ-1D4 | MZ-2A | |
|----------------------|--------------------------------|--------|--------|--------|-------|-------|
| Major elements (%) | SiO ₂ | 57.20 | 56.01 | 57.13 | 46.34 | 57.02 |
| | TiO ₂ | 0.54 | 0.49 | 0.53 | 0.45 | 0.55 |
| | Al ₂ O ₃ | 19.44 | 19.33 | 19.48 | 16.06 | 21.64 |
| | Fe ₂ O ₃ | 2.08 | 3.08 | 2.09 | 6.28 | 4.82 |
| | MnO | 0.05 | 0.17 | 0.04 | 0.81 | 0.21 |
| | MgO | 0.81 | 1.19 | 0.79 | 1.09 | 2.48 |
| | CaO | 2.65 | 2.96 | 2.68 | 7.36 | 1.92 |
| | Na ₂ O | 0.70 | 0.99 | 0.70 | 0.96 | 0.23 |
| | K ₂ O | 6.08 | 5.06 | 6.12 | 5.08 | 3.18 |
| | P ₂ O ₅ | 0.15 | 0.14 | 0.14 | 0.10 | 0.13 |
| | H ₂ O | 8.91 | 9.41 | 8.88 | 14.04 | 7.83 |
| Trace elements (ppm) | Ni | 2 | 4 | 3 | 4 | 7 |
| | P | 660 | 610 | 610 | 430 | 580 |
| | S | 1,100 | 1,090 | 1,090 | 830 | <50 |
| | Sc | 2 | 1 | 2 | 2 | 2 |
| | Ti | 3,150 | 2,820 | 3,040 | 2,590 | 3,160 |
| | V | 121 | 104 | 116 | 92 | 123 |
| | Zn | 117 | 96 | 126 | 89 | 177 |
| | Ag | <0.1 | <0.1 | <0.1 | <0.1 | <0.1 |
| | As | 5 | 4 | 5 | 3 | 2 |

| Sample Code | MZ-1D1 | MZ-1D2 | MZ-1D3 | MZ-1D4 | MZ-2A | |
|----------------------|--------|--------|--------|--------|--------|-------|
| Trace elements (ppm) | Ba | >5,000 | >5,000 | >5,000 | >5,000 | 2,590 |
| | Be | 4.2 | 4.1 | 3.9 | 4.8 | 4.1 |
| | Bi | 0.45 | 0.43 | 0.45 | 0.38 | 0.43 |
| | Cd | 0.41 | 0.32 | 0.39 | 0.29 | 0.24 |
| | Co | 6 | 6 | 6 | 7 | 12 |
| | Cs | 12.6 | 9 | 12.9 | 11.2 | 7.4 |
| | Ga | 18.5 | 19.4 | 19.2 | 16.1 | 19 |
| | Ge | 1.1 | 0.8 | 1.2 | 0.8 | 1.1 |
| | Hf | 5 | 4.5 | 4.8 | 4.2 | 4.2 |
| | In | <0.05 | 0.05 | <0.05 | <0.05 | <0.05 |
| | Li | 2.1 | 1.7 | 2.1 | 1.8 | 1.7 |
| | Mo | 1 | 0.7 | 1.2 | 0.6 | 0.3 |
| | Nb | 6.3 | 5.6 | 6.1 | 5.4 | 5.7 |
| | Pb | 71 | 63 | 67 | 54 | 61 |
| | Rb | 350 | 253 | 285 | 268 | 132 |
| | Re | <0.05 | <0.05 | <0.05 | <0.05 | <0.05 |
| | Sb | 0.7 | 0.5 | 0.7 | 0.6 | 0.3 |
| | Se | 1 | <1 | 2 | 1 | 1 |
| | Sn | 1.8 | 1.6 | 1.9 | 1.6 | 1.8 |
| | Sr | 2,140 | 1,760 | 2,100 | 1,800 | 860 |
| | Ta | 0.54 | 0.49 | 0.52 | 0.44 | 0.48 |
| | Te | <0.1 | <0.1 | <0.1 | 0.1 | <0.1 |
| | Th | 16.4 | 14.4 | 15.7 | 11.9 | 15.3 |
| | Tl | 0.88 | 0.53 | 0.81 | 0.5 | 0.44 |
| | U | 6.14 | 5.39 | 6.09 | 6.13 | 3.93 |
| | W | 0.6 | 0.5 | 0.8 | 2.3 | 0.5 |
| | Y | 25.7 | 17.7 | 25.3 | 47.8 | 23.6 |
| | Zr | 193 | 170 | 187 | 172 | 159 |
| | Ce | 83.4 | 75.6 | 78 | 53.7 | 77.3 |
| | Dy | 5.1 | 3.5 | 4.9 | 6.4 | 4.6 |
| | Er | 2.6 | 1.7 | 2.6 | 4.5 | 2.5 |
| | Eu | 6.6 | 5.9 | 6.4 | 6.1 | 2.3 |
| Gd | 7.7 | 6.2 | 7.4 | 7 | 6.7 | |
| Ho | 0.9 | 0.6 | 0.9 | 1.3 | 0.8 | |
| La | 40.1 | 37.3 | 37.9 | 27.1 | 38.6 | |
| Lu | 0.34 | 0.27 | 0.35 | 0.77 | 0.34 | |
| Nd | 36.3 | 32.3 | 34.3 | 25.1 | 32.9 | |
| Pr | 8.89 | 8.03 | 8.35 | 6.02 | 8.11 | |
| Sm | 7.3 | 5.7 | 7.1 | 5.9 | 6.4 | |
| Tb | 0.88 | 0.63 | 0.85 | 0.94 | 0.75 | |
| Tm | 0.3 | 0.2 | 0.3 | 0.6 | 0.3 | |
| Yb | 2.4 | 1.7 | 2.2 | 4.5 | 2.2 | |

are enriched. In the porphyritic rhyolite host (samples MZ-1D1, MZ-1D2, MZ-1D3, and MZ-1D4) the average Al_2O_3 content is 18.58% and K_2O is 5.59%. These values are higher than the average values of the two major elements in common rhyolite, which are 13.1% for Al_2O_3 and 4.67% for K_2O , respectively (Christiansen et al. 1986). Similarly, in the tuff host (sample MZ-2A), the Al_2O_3 content is 21.64% and K_2O is 3.18%. These values are much higher than the average values of these two elements in common tuff, which are 4.59% for Al_2O_3 and 1.3% for K_2O , respectively (Edris et al. 2021). The significant enrichment of these two elements indicates the presence of zeolite minerals in the two volcanic rocks in the study area.

The water (H_2O) content in all samples also showed high values, specifically 7.83% to 14.04%. Therefore, the sample has reached a temperature in which all volatiles are eliminated, this includes moisture water plus bound water in micas, amphiboles, epidote, and in some which is produced by decomposition of carbonates (calcite and smectite) and also this shows that an alteration process has occurred in the rocks hosting the zeolite mineralization. Fresh igneous and volcanic rocks generally have less than 2% H_2O , whereas if the water content is more than 2%, the rock is classified as altered rock (Le Bas et al. 1986). This shows that the formation of zeolites in the host rocks is caused by an alteration process, as has been shown in the microscopic appearance in petrographic studies (Figure 5).

Using the major elements, when plotted on the Na – (Ca + Mg) – K classification diagram for zeolites (Coombs et al. 1997), in general the samples are distributed in the zeolite-K field (Figure 7). It can therefore be concluded that based on their mineralogy and chemical composition, the type of zeolite in the study area is phillipsite-K (potassium phillipsite).

The potassic character of the host rocks carrying zeolite as well as the high-K character of the zeolite itself is also indicated by the SiO_2 – K_2O plot (Peccerillo and Tay-

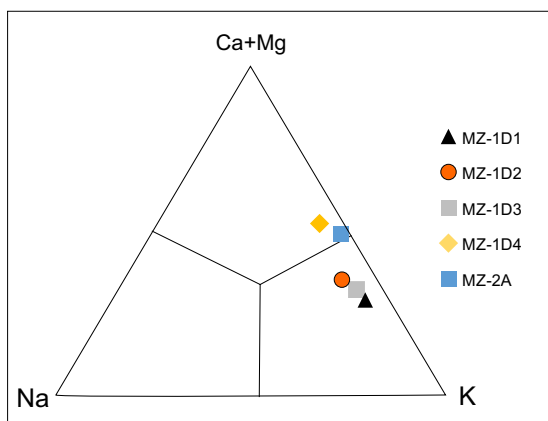


Fig. 7. Na – (Ca + Mg) – K plot of zeolites

Rys. 7. Wykres Na – (Ca + Mg) – K zeolitów

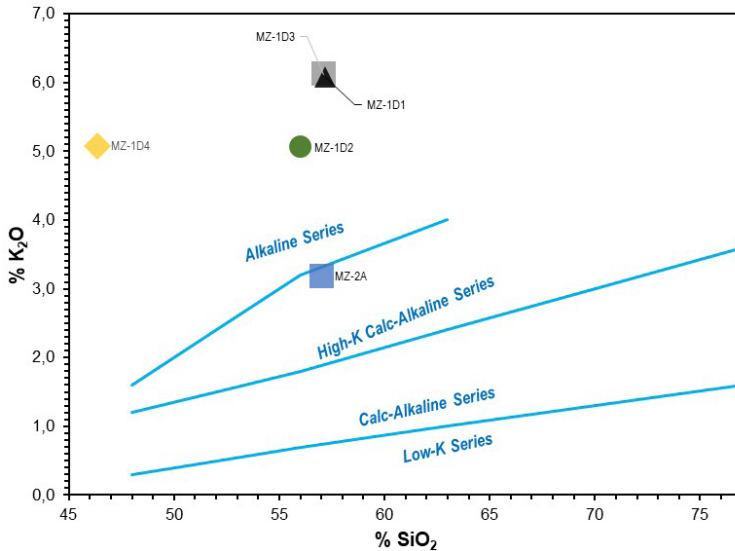


Fig. 8. Plots of the zeolite-bearing volcanic rock samples in the $\text{SiO}_2\text{-K}_2\text{O}$ diagram (Peccerillo and Taylor 1976)

Rys. 8. Wykresy próbek skał wulkanicznych zawierających zeolit na diagramie $\text{SiO}_2\text{-K}_2\text{O}$

lor 1976), where most of the samples are distributed in the alkaline (high-K) series field (Figure 8).

After being normalized to a chondrite composition, the trace elements in the spider diagram are generally enriched in the large ion lithophile elements, LILE (Cs, Rb, Ba, K, Sr, Eu) and depleted in the high field strength elements, HFSE (Nb, Ti, Zr, P) (Figure 9). The enrichment of LILE indicates alteration processes; the enrichment of K and Sr may correspond to the potassic character of the zeolite, while the depletion of HFSE, particularly Zr and Ti, are indications of subduction zone magma (Pearce 1982).

The REE patterns show a general steeply inclined pattern of the light REE (LREE) and medium REE (MREE), and tend to flat in the heavy REE (HREE) (Figure 10), which indicates intermediate to acid composition of the magma (Kamber et al. 2002; Sanematsu et al. 2009). The strong anomaly of Eu indicates that feldspar was added during magma differentiation (Singh and Vallinayagam 2012), where this is consistent with the abundance of feldspar identified in the hand specimen samples and petrography analysis (Figure 4, 5).

2.3. Genesis

Zeolite generally occurs as a result of the reaction between the glassy components of pyroclastic products and fluids. In this regard, a number of factors can influence the zeolitization process:

- ◆ chemistry of the fluids involved (pH, Eh, K/Na);
- ◆ the composition of the rock and the abundance of glassy components such as shards and pumice;
- ◆ physical parameters such as temperature, pressure, the reaction interval between fluid and glass, and the porosity and permeability of the rock.

Zeolitization commonly occurs as a result of the devitrification of the volcanic glass found within glassy pyroclastic deposits, especially under the presence of volatiles and fluids. The devitrification of volcanic glass is known to form zeolite and clay minerals, especially bentonites which contain abundant amounts of dioctahedral smectites (Cicerali et al. 2020).

Most zeolite deposits are genetically associated with Cenozoic volcanic and volcanoclastic units (Cicerali et al. 2020; Mormone and Piochi 2020; Suliman et al. 2022). As described, zeolite mineralization in the study area occurs in the tuff member (porphyritic rhyolite and green tuff) of the Camba Formation. The Camba Formation is composed of sedimentary rocks interbedded with volcanics, which were deposited in the marine environment during the Middle to Late Miocene (Sukamto and Supriatna 1982).

It can be concluded that zeolite mineralization in the Moncongloe area was formed through the following processes. During the Middle to Late Miocene, volcanic activity occurred which deposited porphyritic rhyolite and green tuff in the marine environment together with other volcanic and sedimentary units which were interbedded with each other as found in the outcrop of the stratigraphic sequence in the study area (Figure 3). The porphyritic rhyolite and green tuff then underwent an alteration process due to the interaction between their constituent minerals, namely K-feldspar phenocrysts as well as fine crystalline groundmass and volcanic glass, with hydrothermal fluid, in the alkaline seawater condition.

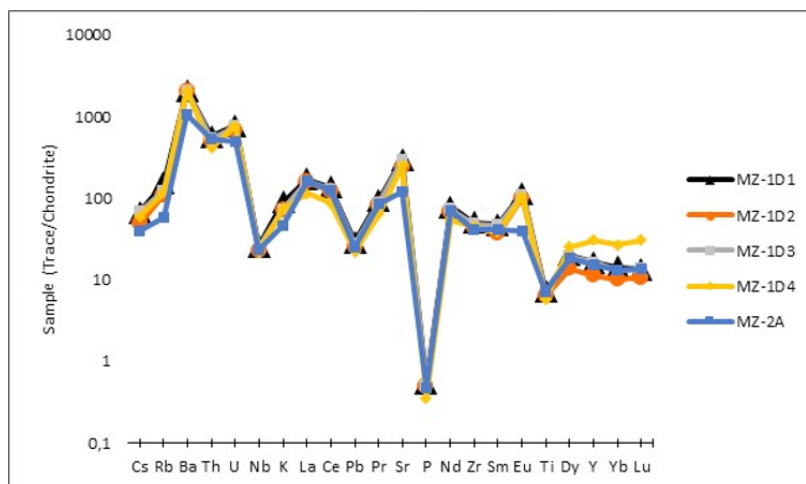


Fig. 9. Trace elements spider diagram

Rys. 9. Wykres pająkowy pierwiastków śladowych

Phillipsite-type zeolite mineral is then formed from the alteration of K-feldspar phenocrysts, which is accompanied by smectite which is formed from the alteration of fine crystalline groundmass and volcanic glass (Figure 5). The presence of phillipsite-type zeolite with smectite was also identified from the XRD analysis (Figure 6). This kind of association between zeolite and smectite is commonly found in various zeolite deposits in many places in the world (e.g., Albayrak and Ozguner 2013; Cicerali et al. 2020).

Major element characteristics, such as enrichment of Al_2O_3 and K_2O , also support the presence of zeolite mineral in the analyzed samples, as explained in subsection 3.2. The type of zeolite in the study area, namely phillipsite, besides being identified from petrographic and XRD analysis (Figure 5 and 6), has also been analyzed based on its chemical characteristics, such as the high content of K_2O (Tabel 1), plot on the $Na - (Ca + Mg) - K$ diagram (Coombs et al. 1997; Figure 7), plot on the $SiO_2 - K_2O$ diagram (Peccerillo and Taylor 1976; Figure 8), and the enrichment of K in the trace elements spider diagram (Figure 9). The high concentration of MgO from the results of chemical analysis (0.79 to 2.48 wt%; Table 1), represent the presence of smectite in the samples. The MgO that is necessary for the formation of smectite can be supplied from the entry of seawater (alkaline) fluids in to the circulation inside the host rocks (Albayrak and Ozguner 2013). The hydrothermal alteration process which is responsible for the formation of zeolite in the study area, is indicated by several facts from the study results, such as the appearance of K-feldspar phenocrysts which are altered to zeolite (Figure 5), the high H_2O content in all samples, ranging from 7.83% to 14.04%, which is far above the average fresh rock content at 2% (Le Bas et al. 1986), and the enrichment of LILE in the trace elements spider diagram (Figure 9).

The hydrothermal fluid which is an important agent of the alteration process responsible for the formation of zeolite in the study area most likely originates from magma intrusion,

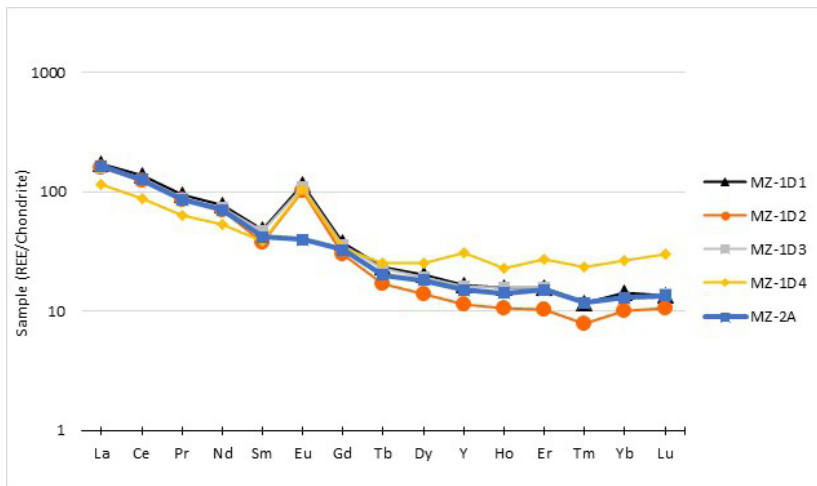


Fig. 10. Rare earth elements (REE) patterns

Rys. 10. Wzorce pierwiastków ziem rzadkich (REE)

which forms basaltic igneous rocks, which are widely distributed in a general direction almost northwest-southeast to northeast-southwest around the study area (Figure 1). These basalt dykes intruded the Camba Formation during the Late Miocene to Pliocene (Sukanto and Supriatna 1982). Thus, it can be concluded that the hydrothermal alteration process in the two volcanic rocks which formed the zeolite mineralization in Moncongloe occurred in that time range. The magma that forms the volcanic rock which is the host of the zeolite mineral is an alkaline series magma (Peccerillo and Taylor 1976; Figure 8) which has an intermediate to acid composition (Kamber et al. 2002; Sanematsu et al. 2009; Figure 10) and originates from subduction zone (Pearce 1982; Figure 9).

The zeolite mineralization that was found in volcanic rock types of porphyritic rhyolite and green tuff, exposed in the Moncongloe area of Maros Regency have a total thickness of 6.8 m (Figure 2, 3) are distributed in nearly west-east strike and have a very gently slope, dipping to the north (N275°E/2°; Figure 2). Thus, for further exploration, it is recommended to conduct mapping to the north, remaining in the Camba Formation.

2.4. Potential utilization

To date, more than forty species of natural zeolites and 253 synthetic zeolites have been recognized. As described in the introduction, zeolite minerals can be used in various applications based on their three specific mineralogical-chemical characteristics, namely absorbers, ion exchangers, and molecular sieves. Based on this, zeolite minerals can generally be used in the fields of agriculture and plantation, farming and fisheries, gas drying and purification, filler, ceramic material, coal gasification, petroleum industry, utilization of solar energy, environmental sustainability, aircraft industry, water purification, photography, and in radioactive fields (Suwardi 2002; Auerbach et al. 2003; Erdem et al. 2004; Moshoeshoe et al. 2017).

This study shows that the zeolite type in Moncongloe area is phillipsite, with the specification of K-phillipsite (K-rich phillipsite). Specifically, phillipsite can be used, inter alia, to remove lead from water (Pansini et al. 1996), to remove paraquat from wastewater (Ibrahim and Jbara 2009), to extract potassium from seawater (Hou et al. 2013), to remove thorium from carbonate solutions (Misaelides et al. 2014), as a catalyst in knoevenagel condensation (Pawaiyaa et al. 2014), in dietary supplementation for pets (Superchi et al. 2017), to uptake ammonia in water (Novembre et al. 2022) and in colorectal cancer therapy (Altoom et al. 2022).

Conclusions

This study concludes that the host rocks of zeolite mineralization in Moncongloe area are porphyritic rhyolite and green tuff, which are volcanic members of the Tertiary Camba Formation. The total thickness of the zeolite-bearing rock layers is 6.8 meters, with a strike of

the layers trending west-east and a dip of 2° to the north (N275°E/2°). Microscopic and XRD studies indicate that the zeolite is of a phillipsite type, which is associated with smectite and was formed as an alteration product of the primary K-feldspar phenocrysts as well as fine crystalline ground mass and volcanic glass. The presence of phillipsite-type zeolite associated with smectite in the studied samples were also confirmed by their chemical compositions, both major- and trace elements, as well as the REE, covering the high concentration of K_2O and MgO , plots of the $Na - (Ca + Mg) - K$ and $SiO_2 - K_2O$ diagrams as well as the K enrichment in the trace elements spider diagram.

Zeolite mineralization associated with smectite in the study area were genetically formed by the alteration process due to the interaction between their constituent minerals – K-feldspar phenocrysts as well as fine crystalline groundmass and volcanic glass, with hydrothermal fluid, in alkaline seawater conditions. The hydrothermal fluid most likely originates from magma intrusion that forms basaltic igneous rocks, which intruded the Camba Formation (including the volcanic host rocks of the zeolite mineralization) during Late Miocene to Pliocene. Thus, it can be concluded that the hydrothermal alteration occurred in that time range. The magma that forms the volcanic host rocks is an alkaline series magma, intermediate to acid in composition, and originating from the subduction zone.

The distribution of volcano-sedimentary rocks member of the Camba Formation in South Sulawesi is very wide. Further research still needs to be done to map the distribution of zeolite deposits in this area.

The authors wish to express a sincere gratitude to the Head of Institute for Research and Community Service Hasanuddin University (LP2M UNHAS), Indonesia, for the financial support through the “2023 Collaborative Fundamental Research Grant”.

REFERENCES

- Albayrak, M. and Ozguner, A.M. 2013. Geology and diagenesis of a zeolitic Foca tuff unit deposited in a Miocene phreatomagmatic lacustrine environment (western Anatolia). *Turkish Journal of Earth Sciences* 22, pp. 611–631, DOI: 10.3906/yer-1203-11.
- Altoom et al. 2022 – Altoom, N., Ibrahim, S.M., Othman, S.I., Allam, A.A., Alqhtani, H.A., Al-Otaibi, F.S. and Abukhadra, M.R. 2022. Characterization of β -cyclodextrin/phillipsite (β -CD/Ph) composite as a potential carrier for oxaliplatin as therapy for colorectal cancer; loading, release, and cytotoxicity. *Colloid and Surfaces A: Physicochemical and Engineering Aspects* 648(8), pp. 129–144, DOI: 10.1016/j.colsurfa.2022.129144.
- Asselman et al. 2022 – Asselman, K., Pellens, N., Thijs, B., Doppelhammer, N., Haouas, M., Taulelle, F., Martens, J.A., Breynaert, E. and Kirschhock, C.E.A. 2022. Ion-pairs in aluminosilicate-alkali synthesis liquids determine the aluminium content and topology of crystallizing zeolites. *Chemistry of Materials* 34(16), pp. 7150–7158, DOI: 10.1021/acs.chemmater.2c00773.
- Auerbach et al. 2003 – Auerbach, S.M., Carrado, K.A. and Dutta, P.K. (eds.), 2003. *Handbook of zeolite science and technology*. New York: Marcel Dekker, Inc., 302 pp., DOI: 10.1201/9780203911167.
- Buzimov et al. 2018 – Buzimov, A.Y., Kulkov, S.N., Gomze, L.A., Geber, R. and Kocserha, I. 2018. Effect of mechanical treatment on the structure and properties of natural zeolite. *Inorganic Materials: Applied Research* 9, pp. 910–915, DOI: 10.1134/S2075113318050040.

- Christiansen et al. 1986 – Christiansen, E.H., Sheridan, M.F. and Burt, D.M. 1986. The geology and geochemistry of Cenozoic topaz rhyolites from the Western United States. *The Geological Society of America Special Paper* 205, pp. 1–82, DOI: 10.1130/SPE205-p1.
- Cicerali et al. 2020 – Cicerali, D., Arslan, M., Yazar, E.A., Yucel, C., Temizel, I., Park, S. and Schroeder, P.A. 2020. Mineralogy, chemistry and genesis of zeolitization in Eocene tuffs from the Bayburt area (NE Turkey): Constraints on alteration processes of acidic pyroclastic deposits. *Journal of African Earth Sciences* 162, pp. 1–14, DOI: 10.1016/j.jafrearsci.2019.103690.
- Coombs et al. 1997 – Coombs, D.S., Alberti, A., Armbruster, T., Artioli, G., Colella, C., Galli, E., Grice, J.D., Liebau, F., Minato, H., Nickel, E.H., Passaglia, E., Peacor, D.R., Quartieri, S., Rinaldi, R., Ross, M., Shepard, R.A., Tillmanns, E. and Vezzalini, G. 1997. Recommended nomenclature for zeolite minerals: report of the subcommittee on zeolites of the international mineralogical association, commission on new minerals and mineral names. *The Canadian Mineralogist* 35(6), pp. 1571–1606.
- Edris et al. 2021 – Edris, W.F., Abdelkader, S., Salama, A.H.E. and Al Sayed, A.A.A. 2021. Concrete behaviour with volcanic tuff inclusion. *Civil Engineering and Architecture* 9(5), pp. 1434–1441, DOI: 10.13189/cea.2021.090516.
- Erdem et al. 2004 – Erdem, E., Karapinar, N. and Donat, R. 2004. The removal of heavy metal cations by natural zeolites. *Journal of Colloid and Interface Science* 280, pp. 309–314, DOI: 10.1016/j.jcis.2004.08.028.
- Hou et al. 2013 – Hou, J., Yuan, J., Xu, J., Fu, Y. and Meng, C. 2013. Template-free synthesis and characterization of K-phillipsite for use in potassium extraction from seawater. *Particuology* 11(6), pp. 786–788, DOI: 10.1016/j.partic.2013.02.003.
- Ibrahim, K.M. and Jbara, H.A. 2009. Removal of paraquat from synthetic wastewater using phillipsite-faujasite tuff from Jordan. *Journal of Hazardous Materials* 163(1), pp. 82–86, DOI: 10.1016/j.jhazmat.2008.06.109.
- Kamber et al. 2002 – Kamber, B.S., Ewart, A., Collerson, K.D., Bruce, M.C. and McDonald, G.D. 2002. Fluid-mobile trace element constraints on the role of slab melting and implications for Archaean crustal growth models. *Contributions to Mineralogy and Petrology* 144(1), pp. 38–56, DOI: 10.1007/s00410-002-0374-5.
- Le Bas et al. 1986 – Le Bas, M.J., Le Maitre, R.W., Streckeisen, A. and Zanettin, B. 1986. A chemical classification of volcanic rocks based on the total alkali-silica diagram. *Journal of Petrology* 27(3), pp. 745–750, DOI: 10.1093/petrology/27.3.745.
- McDonough, W. and Sun, S.S. 1995. The composition of the Earth. *Chemical Geology* 120(3–4), pp. 223–253, DOI: 10.1016/0009-2541(94)00140-4.
- Misaelides et al. 2014 – Misaelides, P., Gaona, X., Altmaier, M. and Geckies, H. 2014. Thorium removal from carbonate solutions by HDTMA-modified HEU-type zeolite-, chabazite- and phillipsite-bearing tuffs. *Proceedings of the 9th International Conference on the Occurrence, Properties and Utilization of Natural Zeolites*, June 2014, Belgrade, Serbia.
- Mormone, A. and Piochi, M. 2020. Mineralogy, geochemistry and genesis of zeolites in Cenozoic pyroclastic flows from the Asuni area (Central Sardinia, Italy). *Minerals* 10(3), DOI: 10.3390/min10030268.
- Moshoeshoe et al. 2017 – Moshoeshoe, M., Nadiye-Tabbiruka, M.S. and Obuseng, V. 2017. A review of the chemistry, structure, properties and applications of zeolites. *American Journal of Materials Science* 7(5), pp. 196–221, DOI: 10.5923/j.materials.20170705.12.
- Novembre et al. 1986 – Novembre, D., Gimeno, D., Calista, M., Mancinelli, V. and Miccadei, E. 2022. On the suitability of phillipsite-chabazite zeolite rock for ammonia uptake in water: a case study from the Pescara River (Italy). *Scientific Reports* 12, DOI: 10.1038/s41598-022-13367-y.
- Pansini et al. 1986 – Pansini, M., Colella, C., Caputo, D., de Gennaro, M., Langella, A. 1996. Evaluation of phillipsite as cation exchanger in lead removal from water. *Microporous Materials* 5(6), pp. 357–364, DOI: 10.1016/0927-6513(95)00071-2.
- Pawaiyaa et al. 1986 – Pawaiyaa, P., Pawaiya, A., Agrawai, N. and Tomar, R. 2014. An efficient knoevenagel condensation using phillipsite zeolite as catalyst in liquid phase under solvent free condition. *International Journal of Chemical and Pharmaceutical Analysis* 1(3), pp. 115–120.
- Pearce, J. 1982. *Trace element characteristics of lavas from destructive plate boundaries*. [In:] Thorpe, R.S. ed. *Andesites: Orogenic Andesites and Related Rocks*. John Wiley and Sons, pp. 525–548.
- Peccerillo, A. and Taylor, S.R. 1976. Geochemistry of Eocene calc-alkaline volcanic rocks from the Kastamonu area, northern Turkey. *Contributions to Mineralogy and Petrology* 58, pp. 63–81, DOI: 10.1007/BF00384745.

- Pellens et al. 2022 – Pellens, N., Doppelhammer, N., Asselman, K., Thijs, B., Jakoby, B., Reichel, E.K., Taulelle, F., Martens, J.A., Breynaert, E. and Kirschhock, C.E.A. 2022. A zeolite crystallisation model confirmed by in situ observation. *Faraday Discussions* 235, pp. 162–182, DOI: 10.1039/D1FD00093D.
- Sanematsu et al. 2009 – Sanematsu, K., Murakami, H., Watanabe, Y., Duangsurigna, S. and Vilayhack, S. 2009. Enrichment of rare earth elements (REE) in granitic rocks and their weathered crusts in central and southern Laos. *Bulletin of the Geological Survey of Japan* 60(11), pp. 527–558, DOI: 10.9795/bullgsj.60.527.
- Singh, L.G. and Vallinayagam, G., 2012. Petrological and geochemical constraints in the origin and associated mineralization of A-type granite suite of the Dhiran area, Northwestern Peninsular India. *Geosciences* 2(4), pp. 66–80, DOI: 10.5923/j.geo.20120204.02.
- Sukanto, R. and Supriatna, S. 1982. Geologic map of the Ujung Pandang, Benteng and Sinjai quadrangles, Sulawesi. *Geological Research and Development Centre, Bandung, Indonesia*.
- Suliman et al. 2022 – Suliman, T.A., Eshag, T.E., Hassan, M.A. and Kotelnikov, A.E. 2022. Mineralogy and genesis of zeolites of Gedarif area, Eastern Sudan. *IOP Conference Series: Earth and Environmental Science* 988, DOI: 10.1088/1755-1315/988/4/042061.
- Superchi et al. 2017 – Superchi, P., Saleri, R., Ossiprandi, M.C., Riccardi, E., Passaglia, E., Cavalli, V., Beretti, V. and Sabbioni, A. 2017. Natural zeolite (chabazite/phillipsite) dietary supplementation influences faecal microbiota and oxidant status of working dogs. *Italian Journal of Animal Science* 16(1), pp. 115–121, DOI: 10.1080/1828051X.2016.1261008.
- Suwardi, 2002. Prospects for the Use of Zeolite Minerals in Agriculture (*Prospek Pemanfaatan Mineral Zeolit di Bidang Pertanian*). *Jurnal Zeolit Indonesia* 1(1), pp. 5–12 (in Indonesian).

**THE GENESIS AND POTENTIAL UTILIZATION OF ZEOLITE
IN THE MONCONGLOE AREA, MAROS, SOUTH SULAWESI, INDONESIA**

Keywords

utilization, zeolite, alteration, phillipsite, Moncongloe

Abstract

In Moncongloe area, Maros Regency, South Sulawesi Province, Indonesia, zeolite mineralization in porphyritic rhyolite and green tuff was identified occurred in a volcano-sedimentary sequence, members of the Miocene Camba Formation. This paper describes a recent study of the zeolite mineralization on the basis of field and laboratory data, which focused on its genetic aspects and potential utilizations based on its mineralogical and chemical characteristics. The laboratory works applied in this study include mineralogical analysis (petrography and XRD) and bulk chemical analysis (XRF for major oxides, ICP-OES and ICP-MS for trace elements). Microscopic and XRD studies indicate that the zeolite is a phillipsite type, which is associated with smectite, and was formed as an alteration product of the primary K-feldspar phenocrysts as well as fine crystalline ground mass and volcanic glass. The presence of phillipsite-type zeolite associated with smectite were also confirmed by the chemical compositions. The zeolite mineralization associated with smectite in the study area were formed by alteration process by hydrothermal fluid in alkaline seawater condition, during Late Miocene to Pliocene. So, it can be concluded that the hydrothermal alteration is occurred in that time range. The magma that forms the volcanic host rocks is an alkaline series magma, intermediate to acid in composition, and originates from subduction zone. The K-rich phillipsite-type zeolite in the

study area can be used for, among other things: to remove lead from water, remove paraquat from wastewater, extract potassium from seawater, remove thorium from carbonate solutions, as catalyst in Knoevenagel, as dietary supplementation for pets, to uptake ammonia in water, and for colorectal cancer therapy.

GENEZA I POTENCJALNE WYKORZYSTANIE ZEOLITU NA OBSZARZE MONCONGLOE, MAROS, SULAWESI POŁUDNIOWE, INDONEZJA

Słowa kluczowe

wykorzystanie, zeolit, przeróbka, filipsyt, Moncongloe

Streszczenie

Na obszarze Moncongloe w regencji Maros w prowincji Sulawesi Południowej w Indonezji zidentyfikowano mineralizację zeolitu w porfirowym ryolicie i zielonym tufie w sekwencji wulkaniczno-osadowej, należącej do mioceńskiej formacji Camba. W artykule opisano najnowsze badania mineralizacji zeolitu na podstawie danych terenowych i laboratoryjnych, które koncentrowały się na jej aspektach genetycznych i potencjalnych zastosowaniach w oparciu o jej właściwości mineralogiczne i chemiczne. Prace laboratoryjne zastosowane w tym badaniu obejmują analizę mineralogiczną (petrografia i XRD) oraz masową analizę chemiczną (XRF dla głównych tlenków, ICP-OES i ICP-MS dla pierwiastków śladowych). Badania mikroskopowe i XRD wskazują, że zeolit jest typem filipsytu, który jest związany ze smektytem i powstał jako produkt przemiany pierwotnych fenokryształów skałenia K, a także drobnokrystalicznej masy gruntowej i szkła wulkanicznego. Obecność zeolitu typu filipsytowego związanego ze smektytem została również potwierdzona przez skład chemiczny. Mineralizacja zeolitu związana ze smektytem na badanym obszarze powstała w wyniku procesu przemiany przez płyn hydrotermalny w alkalicznej wodzie morskiej, od późnego miocenu do pliocenu. Można zatem stwierdzić, że w tym przedziale czasowym nastąpiły zmiany hydrotermalne. Magma tworząca wulkaniczne skały macierzyste, to magma serii zasadowej, o składzie pośrednim do kwaśnego, pochodząca ze strefy subdukcji. Zeolit typu filipsytu bogaty w K na badanym obszarze może być stosowany m.in. do: usuwania ołowiu z wody oraz parakwatu ze ścieków, ekstrakcji potasu z wody morskiej, usuwania toru z roztworów węglanowych, jako katalizator w Knoevenagelu, a także jako suplement diety dla zwierząt domowych, do wchłaniania amoniaku w wodzie oraz do terapii raka jelita grubego.